

Research paper

Influence of nanomechanical crystal properties on the comminution process of particulate solids in spiral jet mills

Sascha Zügner, Karin Marquardt, Ingfried Zimmermann *

Institute of Pharmaceutical Technology, University of Würzburg, Würzburg, Germany

Received 20 April 2005; accepted in revised form 9 August 2005

Available online 3 October 2005

Abstract

Elastic-plastic properties of single crystals are supposed to influence the size reduction process of bulk materials during jet milling. According to Pahl [M.H. Pahl, *Zerkleinerungstechnik* 2. Auflage. Fachbuchverlag, Leipzig (1993) [1]] and H. Rumpf: [Prinzipien der Prallzerkleinerung und ihre Anwendung bei der Strahlmahlung. Chem. Ing. Tech., 3(1960) 129–135. [2]] fracture toughness, maximum strain or work of fracture for example are strongly dependent on mechanical parameters like hardness (H) and young's modulus of elasticity (E). In addition the dwell time of particles in a spiral jet mill proved to correlate with the hardness of the feed material [F. Rief: Ph. D. Thesis, University of Würzburg (2001)[3]]. Therefore 'near-surface' properties have a direct influence on the effectiveness of the comminution process. The mean particle diameter as well as the size distribution of the ground product may vary significantly with the nanomechanical response of the material. Thus accurate measurement of crystals' hardness and modulus is essential to determine the ideal operational micronisation conditions of the spiral jet mill.

The recently developed nanoindentation technique is applied to examine subsurface properties of pharmaceutical bulk materials, namely calcite, sodium ascorbate, lactose and sodium chloride. Pressing a small sized tip into the material while continuously recording load and displacement, characteristic diagrams are derived. The mathematical evaluation of the force-displacement-data allows for calculation of the hardness and the elastic modulus of the investigated material at penetration depths between 50–300 nm.

Grinding experiments performed with a modified spiral jet mill (Type Fryma JMRS 80) indicate the strong impact of the elastic-plastic properties of a given substance on its breaking behaviour. The fineness of milled products produced at constant grinding conditions but with different crystalline powders varies significantly as it is dependent on the nanohardness and the elasticity of the feed material.

The analysis of this correlation gives new insights into the size reduction process.

© 2005 Elsevier B.V. All rights reserved.

Keywords: Nanoindentation; Elastic-plastic properties; Hardness; Young's modulus; Jet-mill; Impact grinding

1. Introduction

During the past few years there has been an increasing interest in the determination of mechanical parameters of fine

powders in the micron and submicron range. The development of the scanning probe technology in conjunction with improvements in the indentation technique allowed to extend these studies in the nanometer range. It had an immense impact on the field of tribology. Though mainly applied in material science to characterize ultra-thin films or coatings, nanoindentation can also be used to investigate the local mechanical response of crystals in powder technology.

In the theory of comminution elastic-plastic properties of the materials to be ground are of utmost importance as they determine the breaking resistance as well as the formation and propagation of cracks. By this way they define the degree of size reduction [1,2]. Therefore parameters like hardness and young's modulus should have a strong influence on the grindability of the bulk material.

Very often particle sizes in the micron or submicron range are required in the pharmaceutical industry. Efficient jet mills are utilized to obtain such fine products. Despite of

Abbreviations H indentation hardness (GPa); E young's modulus of elasticity (GPa); E_r reduced modulus of elasticity (GPa); P applied load (μN); P_{\max} maximum load (μN); h indentation depth (nm); h_c contact depth (nm); h_{\max} maximum indentation depth (nm); A_c projected area of contact (nm^2); $f(h_c)$ indenter shape function; $S = dP/dh$ contact stiffness ($\mu\text{N}/\text{nm}$); AFM atomic force microscope; ε geometric constant (0.75 for Berkovich diamond indenter); ν poisson ratio (ν for diamond=0.07); C_1 – C_5 area function coefficients; d -value x -value, where $Q_3(x) = 0.632$ (taken from RRSB diagram); n -value slope of the RRSB straight lines.

* Corresponding author. University of Würzburg, Institute of Pharmaceutical Technology, Am Hubland D-97074 Würzburg, Germany. Tel.: +931 8885470; fax: +931 8884608.

E-mail address: zimmerm@pzl.uni-wuerzburg.de (I. Zimmermann).

the intensive use and enforced research the detailed mechanism of impact grinding is not yet entirely understood. Therefore and as various mechanical parameters affect this operation, it cannot be fully controlled up to date.

In this work hardness and modulus values are determined on a nanoscale. These features highly influence the comminution process. The correlation of elastic-plastic parameters with the particle size distribution of the micronized bulk material will contribute to a better understanding of the comminution process in jet mills in order to control this unit operation.

Indentation technique proves to be an excellent method for the characterization of local mechanical properties on a nanometer scale. By pressing a nanosized diamond tip of well-known shape into a material, applying loads lower than 10 mN, while continuously recording penetration depth with nm-resolution, force-displacement-curves can be obtained. According to the theory developed by Oliver and Pharr [4] the relation between applied load and depth of the resulting indent provides quantitative data of the elastic-plastic response. Surface hardness (H) is defined as maximum load (P_{\max}) divided by the area of contact (A_c) between indenter and sample at maximum load.

$$H = \frac{P_{\max}}{A_c} \quad (1)$$

The contact area A_c is calculated by means of the shape function $A_c = f(h_c)$ of the diamond tip, which describes the cross-sectional area of the indenter at a certain contact depth h_c .

Based on the assumption, that during the initial unloading the area of contact remains constant, Sneddon's analysis [5] of the indentation of an elastic half-space by a flat, cylindrical punch also describes the indentation by a diamond tip correctly. This leads to the simple relation between load (P) and penetration depth (h):

$$S = \frac{dP}{dh} = \frac{2}{\sqrt{\pi}} * \sqrt{A_c} * E_r \quad (2)$$

By fitting the experimental data of the unloading curve by a power law relation, $S = dP/dh$ can be derived from the slope of its upper portion. The so-called contact stiffness (S) is essential to calculate the reduced modulus of elasticity (E_r) according to Eq. (2).

Nanoindentation has proven to be a reliable method not only to characterize smooth and hard surfaces like coatings, but also to successfully investigate the elastic-plastic properties of rough, non-uniform polycrystals. In this context the combination of the indentation technique with the atomic force microscopy (AFM) allows for additional insights. The three-sided diamond tip which typically is forced into the crystal surface can also be used in a way similar to an AFM cantilever, allowing for an in situ imaging of the area to be studied before and after indenting.

With some materials an increase in penetration depth at peak load can be observed while the force remains constant over a certain period of time. This phenomenon indicates time-dependent plastic effects. The so called indentation creep, a

well-known property of many materials observed at room temperature as well as at elevated temperatures, is believed to be caused by dislocation glide plasticity [6].

With some materials the formation of pile-up around the indent can be observed [7]. This phenomenon is a severe problem in nanoindentation as it leads to false hardness values due to an underestimation of the contact area. Therefore the piled-up material has to be quantified by surface imaging and roughness analyses. In addition another interesting feature has to be considered. With anisotropic crystals the hardness is expected to vary with respect to indenter rotation.

In order to achieve a homogenous distribution within a tablet, drugs often have to be micronized. Jet milling is an efficient technique in reducing the size of crystalline materials. In this study the different bulk materials were comminuted using a spiral jet mill Type Fryma JMRS 80 modified by Rief [3]. The product fineness is the result of a grinding and classifying process. High milling pressures and low feed rates result in high amounts of energy per particle available for breakage processes. Moreover at wide slit width because of a low suction effect out of the grinding chamber particles can be stressed for a long time. Under these conditions finest mill products of narrow particle size distribution are discharged. For sure it is important that the grinding process is reproducible. Therefore the mill is reconstructed in such way that the operational parameters, namely the feed rate, the particle feed pressure, the grinding pressure and the slit width at the vortex finder tube can be adjusted precisely.

Thus pharmaceutical powders with varying elastic-plastic behaviour can be investigated while keeping the important machine parameters almost constant during comminution.

By means of particle size analyses the influence of nanomechanical properties on the product fineness after milling was determined. Subsequently the grinding products were characterized with respect to their particle diameter using the d- and the n-values taken from the RRSB diagram.

Grinding experiments performed with hard and brittle as well as with soft and elastic materials indicate that both hardness and young's modulus strongly affect the size reduction process. While hard and elastic samples require enormous grinding energies, soft and inelastic materials demand only less work of fraction [9].

2. Materials and methods

2.1. Specimen materials

The following substances were included in our studies: the naturally grown but ground calcite 'Criscarb V 130' (Eduard Merkle GmbH&Co. KG, Blaubeuren, Germany), sodium ascorbate Type AG (Hoffmann-LaRoche AG, Basel, Switzerland), lactose 'Prismalac 40' (Meggle GmbH&Co. KG, Wasserburg, Germany) and sodium chloride (Caesar&Loretz, Hilden, Germany). All materials were stored at dry ambient conditions and used as supplied. The crystal structures as well as the gravities of these substances are rather different, Table 1.

Table 1
Physical properties of the test materials

Material	Density [11] [g/cm ³]
Calcite	2.70
Lactose	1.54
Sodium ascorbate	1.78
Sodium chloride	2.17

The densities of the two inorganic materials are significantly higher than those of the two organic materials.

2.2. Sample preparation

Reproducible nanoindentation measurements can be performed only on smooth and almost horizontal surfaces. Therefore particles fulfilling these conditions were selected under a stereomicroscope ('Olympus S11', Olympus Optical Co., Hamburg, Germany).

The selected crystals had to be fixed on the metallic sample support by means of a non-elastic adhesive. In order to avoid that the elastic properties of the adhesive interfere with those of the crystal the latter one must be pressed into the adhesive until it is in direct contact with the metallic sample support. In addition the depths of the indentations were small compared to the mean particle diameters. Thus effects resulting from the ductile adhesive could be eliminated.

The hardening time of the adhesive was long enough to allow for an orientation of the particle such that the slope of its horizontal surface did not exceed 5%. When the adhesive was fully hardened dust and fines adhering on the particle surface were removed by means of compressed air as they might disturb the measurements.

2.3. Indentation procedure

Hardness is generally defined as the resistance of a material against a permanent local deformation when a hard indenter is

pressed into a sample surface. Therefore, it is calculated as the applied load divided by the projected area of contact (Eq. (1)). Depths sensing nanoindentation techniques allow to record simultaneously the applied load as well as the tip displacement during the loading/unloading cycle. Fig. 1 gives a schematic representation of an indentation sequence. In addition it explains how to determine the parameters needed for the evaluation of the experiment. The calculation of hardness and modulus is based on Sneddon's analysis of the elastic contact between a rigid, axisymmetric punch and an isotropic, elastic half space [5].

The peak load (P_{\max}) can be taken directly from the force-depth-curve. According to Oliver and Pharr [4] the contact depth (h_c) which describes the depth of the indent at peak load is calculated as follows:

$$h_c = h_{\max} - \varepsilon \frac{P_{\max}}{S} \quad (3)$$

ε is a geometrical constant associated with the tip shape ($\varepsilon = 0.75$ for a pyramidal Berkovich tip) [4]. Once h_c is determined, the projected contact area (A_c) can be evaluated empirically. For an ideal Berkovich geometry the area function can be expressed as $A_c = f(h_c) = 24.5h_c^2$. Taking into account the imperfectness of the tip which is intensified by its blunting, a modified shape function was introduced:

$$A_c = f(h_c) = 24.5h_c^2 + C_1h_c + C_2h_c^{0.5} + C_3h_c^{0.25} + C_4h_c^{0.125} + C_5h_c^{0.0625} \quad (4)$$

As described below the coefficients (C_1 – C_5) are determined experimentally. A_c , the area of contact, is used to calculate the hardness by means of Eq. (1).

The reduced young modulus (E_r) can be obtained by rewriting Eq. (2). However E_r is a composite value consisting of the young's modulus of the diamond indenter (E_i) as well as that one of the tested material, the specimen's real modulus E_s . Therefore it can be calculated by means of Eq. (5):

$$E_r = \left[\frac{1 - \nu_s^2}{E_s} + \frac{1 - \nu_i^2}{E_i} \right]^{-1} \quad (5)$$

ν_i and ν_s are the Poisson ratios of the indenter (diamond) and of the sample respectively.

The combination of nanoindentation and atomic force microscopy (AFM) allows for a proper location of areas being almost horizontal as well as for an in situ-imaging of the particle surface immediately after a plastic indentation is performed. A typical indent mark on a surface of calcite is shown in Fig. 2.

The indentation experiments were performed utilizing a conventional AFM base ('NanoScope® E', Digital Instruments Inc., St Barbara, USA). The microscope laser head was replaced by an add-on force transducer ('TriboScope®', Hysitron Inc., Minneapolis, USA) which generates and measures the indentation force. Simultaneously it controls the z-movement of the tip. The indentation device consists of a

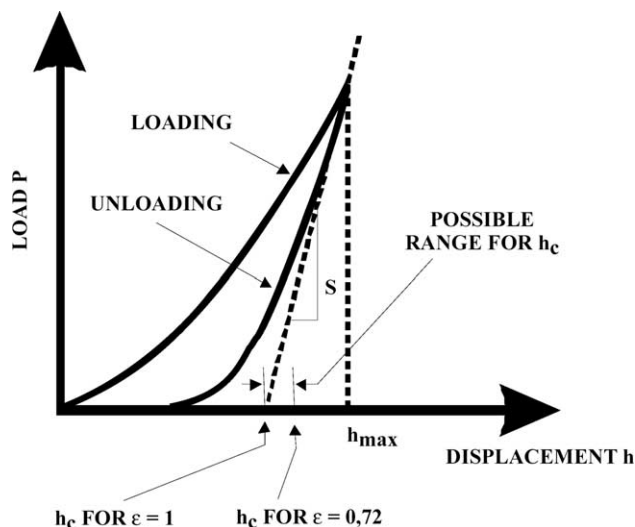


Fig. 1. A typical load–displacement curve showing the essential parameters for the determination of elastic–plastic constants.

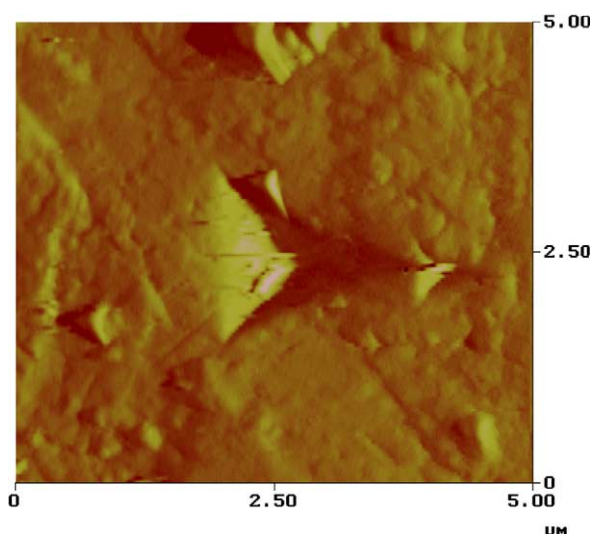


Fig. 2. AFM scan of a typical indent mark on a calcite surface.

three-plate (Be–Cu) capacitive sensor described in detail by Bhushan et al. [12].

The investigations were carried out using a calibrated three-faced diamond tip (=Berkovich) with a total included angle of 142.3° . The tip shape function is given as $A_c = 24.5h_c^2$ for a perfect Berkovich indenter. Due to the blunting of the tip it has to be corrected. For this purpose several indents were performed on fused silica with well-known modulus ($E_r = 69.6$ GPa). The real area function of the indent mark obtained by this way was derived according to the theory of Oliver and Pharr [4].

2.4. Milling experiments

In a spiral jet mill the particles to be ground are stressed by impact. The fineness of the milled products is affected on the one hand by the geometrical and operational parameters of the mill and on the other hand by the mechanical properties of the feed material.

The jet mill used in these experiments was modified by Rief and Marquardt in such a way that operational parameters could

be adjusted precisely [3,8]. A special dosing system ensures that the bulk material can be fed with an adjustable constant feed rate into the milling chamber. Pressure reducing valves allow to adjust the grinding and the feed pressure with a precision of 0.1 bar. By means of a toothed wheel the slit width (=distance between vortex finder tube and the covering of the grinding chamber) can be adjusted with a precision of 1 mm. In order to avoid growth of the crystals of the milled product under the influence of humidity it is collected in a non-solvent liquid. In order to get reliable and reproducible information, the milling process has to be validated. For this reason grinding experiments and measurements of particle size distributions of the product were performed repeatedly. It could be shown, that the results did not differ significantly. A diagram of the experimental setup of the reconstructed Fryma JMRS 80 is given in Fig. 3.

It was the aim of our study to investigate the influence of elastic–plastic properties on the breaking behaviour during impact grinding. Therefore, all operational and geometrical parameters of the mill were kept constant while the four model substances with varying nanomechanical properties were comminuted.

After each milling by means of Coulter LS laser diffraction technology a particle size analysis of the ground material was performed. The milled products were characterized by their d - and n -values taken from the RRSB diagram.

By comparing the product fineness of different materials at constant operational parameters it should be possible to detect the influence of mechanical properties on the grinding and classifying process. A milling product characterized by small particle sizes would indicate that the low hardness of the material is determining the result. However, if the elastic modulus is the determining factor high d -values should be expected.

In order to better understand the processes in the spiral jet mill, they must be described quantitatively. To this end correlation analyses between the operational parameters of the mill and the d - and n -values of the particle size distributions of the ground materials were performed. The elastic–plastic

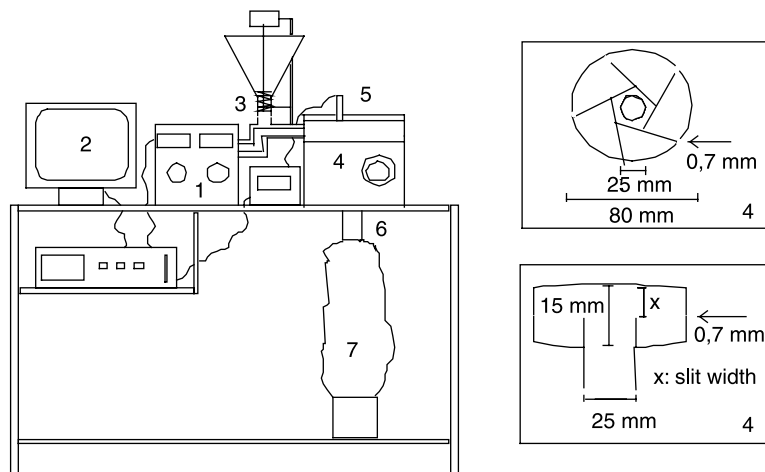


Fig. 3. Modified spiral jet mill Type Fryma JMRS 80. 1: Pressure reducing valves and manometer for adjustment of feed and milling pressure; 2: Computer; 3: Dosing system and injector; 4: Milling chamber with dimensions and alignment of the nozzles; 5: Pressure transducer; 6: Vortex finder; 7: Collector.

Table 2
Young's modulus and hardness of the test materials

Material	Young's modulus (mean) [GPa]	Hardness (mean) [GPa]
Calcite	85.9	3.0
Lactose	23.7	1.1
Sodium ascorbate	41.6	1.8
Sodium chloride	46.5	0.44

properties of the materials could be included successfully into our statistical calculations. Models of second order proved to adequately describe the influence of hardness and young's modulus on the fineness of the product.

The substances included in our milling experiments are listed in Table 1. To get comparable and reliable results, the initial grain size of the investigated powders should be almost equal. Therefore we had to take care that the mean particle diameters and the size distributions of the selected bulk materials were similar. According to Ramanujam et al.[10] however slight differences in the particle size of the feed material will not affect the milling result (Table 2).

3. Results and discussion

3.1. Elastic–plastic properties

The unloading and reloading curves of the four substances included in our study do not overlap but form hysteresis loops, Fig. 4. This clearly indicates that such materials show not only elastic but also plastic behaviour. However when multiple loading cycles are performed this effect becomes smaller and smaller. The last unloading curve should be characterized by an elastic behaviour only.

Obviously all tested bulk materials exhibit distinct elastic–plastic behaviour. The load-displacement curves shown in Fig. 4 indicate a marked plastic response. Sodium chloride turns out to be almost entirely plastic. In fact the elastic portion in the unloading curve of NaCl reaches only 5–10%, while the elastic recovery of calcite and sodium ascorbate is about 30–35% during the last unloading. In contrast crystals of lactose are highly elastic as the portion of elastically recovered energy amounts to nearly 50%. It is evident, that for sodium chloride the deformation energy is dissipated by a permanent plastic deformation. This means the indenter mark does not change its shape during unloading. However lactose is able to reversibly store strain energy, which is released during the removal of the indenter. The extent of elasticity seen in the last unloading curves of CaCO_3 , NaCl, Na-ascorbate and lactose has no negative impact on the determination of young's modulus as for this purpose only the linear part of the beginning unloading curve is used.

Since all different crystals in Fig. 4 were loaded with a maximum indentation force of 800 μN the tip displacement gives first qualitative information about nano-hardness.

Calcite showing an indentation depth of only 90 nm is the hardest of the tested materials, while the large displacement with sodium chloride (240 nm) indicates a very soft surface. Lactose and sodium ascorbate having intermediate depths exhibit hardness values between the two extremes. Cross section analyses of the indented sectors carried out using the atomic force feature of the nanoindenter indicated no amounts of pile up so that this effect can be neglected in this study.

Moreover the slope of the unloading portion characterizes the elastic parameter. Therefore sodium chloride should have an extremely high young's modulus compared to its low

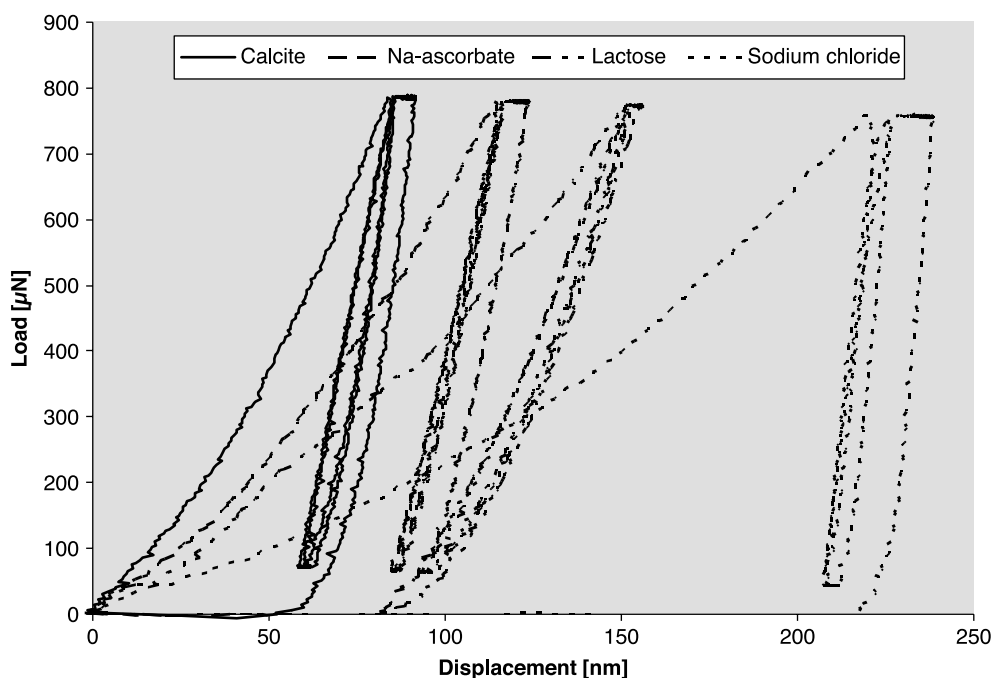


Fig. 4. Load versus indenter displacement of four different crystalline particles at maximum load of 800 μN .

hardness. This fact indicates a soft and brittle material, which should show ideal breaking behaviour. The small slope in the last unloading of lactose results from its low young's modulus. Lactose crystals are highly elastic and thus comminution may require increased energy compared to the other substances.

3.2. Hardness and Young's modulus

As the breaking behaviour is not influenced by the hardness solely, both plastic and elastic parameters have to be taken into account. Detailed evaluation of the given force-displacement-curves yielded the values for plastic hardness and elastic modulus as shown in Fig. 5(a) and (b):

Hardness and young's modulus of the four materials, as determined experimentally, differ strongly (Fig. 5(a) and (b)). Calcite with a particle diameter of 500 μm proves to be the hardest and most brittle substance with $H=2.8\text{--}3.4\text{ GPa}$ and $E=83\text{--}88\text{ GPa}$. As a marked contrast the very plastic, ductile sodium chloride shows a much lower hardness of about 0.41–0.48 GPa, but also a relatively high elastic modulus of 45–48 GPa. Therefore the soft NaCl crystals can easily be deformed. The energy required to grind them should be much smaller than that one needed to crack hard CaCO_3 particles.

For sodium ascorbate a hardness of 1.7–1.9 GPa was determined. The elastic rate during last unloading however is comparable with the recovery of CaCO_3 . The young's modulus

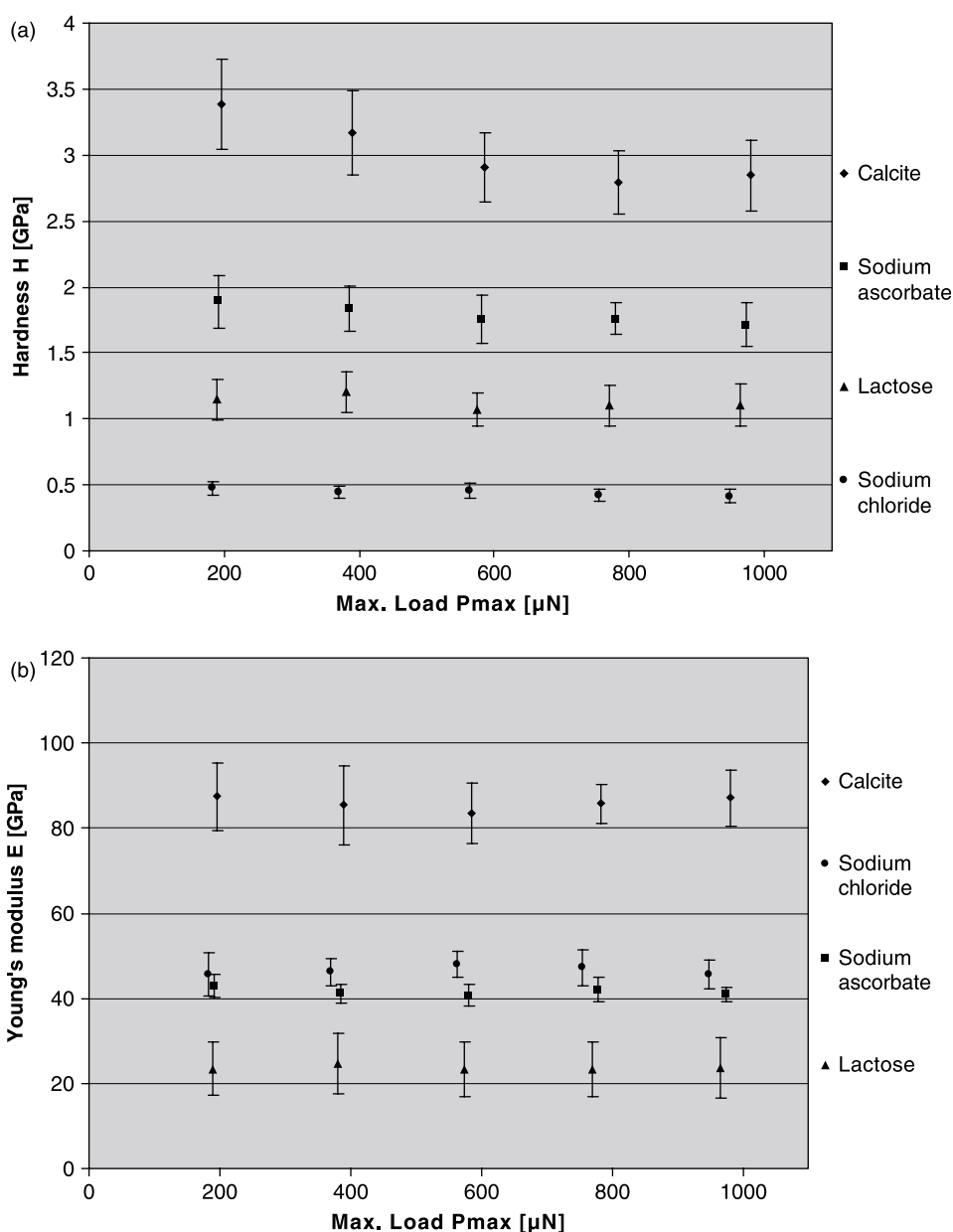


Fig. 5. (a) Mean hardness numbers of four crystalline bulk materials (particle diameter = 500 μm) at different maximum loads (error bars represent one SD). (b) Mean young's modulus of four crystalline bulk materials (particle diameter = 500 μm) at different maximum loads (error bars represent one SD).

of the vitamin C salt amounts to 40–43 GPa. As sodium ascorbate shows similar elastic-plastic behaviour but significant lower hardness than calcite, the comminution in a spiral jet mill at identical operating conditions should result in a milling product being much more fine-grained (d-values).

Lactose proves to be the most elastic of all materials tested in this study ($E=23\text{--}25$ GPa). During unloading more than 45% of the deformation energy is recovered elastically. Lactose on the other hand is a rather soft material. The hardness of crystals with a particle size of $500\text{ }\mu\text{m}$ is characterized by values in a range from 1.0 to 1.2 GPa.

Calcite crystals are intrinsically anisotropic. Therefore it could be expected that the hardness varies with respect to indenter rotation. Despite of its rhombohedral structure hardness and modulus anisotropy for CaCO_3 cannot be observed. In fact the values for H and E measured at indenter

rotation angles of 0° , 30° and 45° are identical within the relatively wide limits of experimental uncertainty. These findings are in a good agreement with theories developed by Simmons and Wang [7]. They suggested that elastic averaging exists in polycrystalline aggregates.

3.3. Influence of the hardness and the Young modulus on the particle comminution

In a jet mill the micronization conditions are determined by their geometrical and operational parameters. The instrumentation of the modified Fryma JMRS 80 allows to adjust and to control all geometrical and operational parameters. If these parameters are kept constant, differences in the fineness of the milling products should only be due to the different mechanical properties of the feed

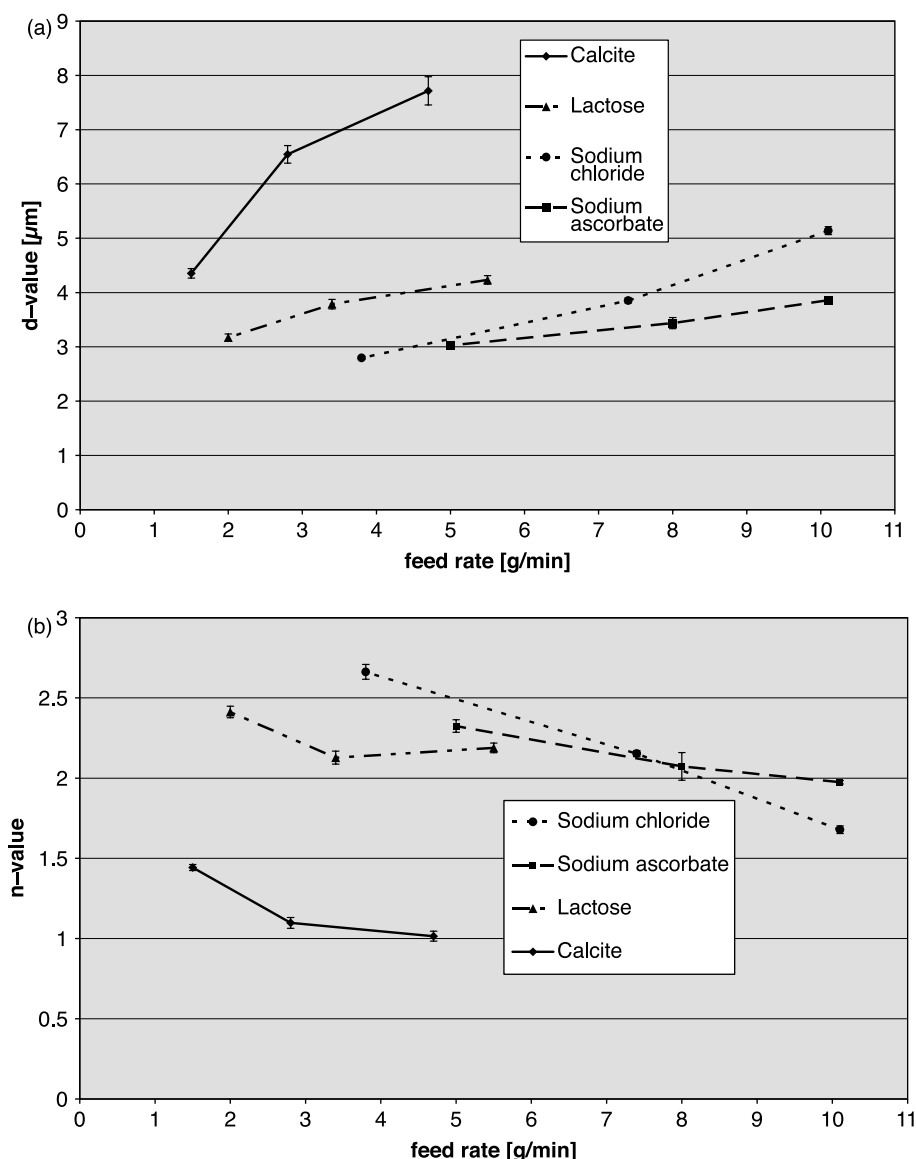


Fig. 6. (a) d-values (taken from RRSB diagrams) of four powders at constant operational parameters. (b) n-values (taken from RRSB diagrams) of four powders at constant operational parameters.

material. In the following two Fig. 6(a) and (b), the variation of the d - and n -values of the particle size distributions of milled products produced at constant grinding conditions (slit width=5 mm, grinding pressure=5 bar) but with different feed materials is shown. Every curve represents a different feed material.

Obviously the four bulk materials differ significantly in their breaking behaviour. Even though every experiment was conducted under identical conditions the particle sizes of the ground products vary distinctly.

Above all the hardest and most brittle calcite exhibits the highest d -values and the lowest n -values indicating large particle sizes and wide size distributions. Mainly due to its hardness CaCO_3 requires for high milling energies to be sufficiently comminuted.

Considering the data of lactose it is evident that not only the plastic parameter hardness but also the elastic modulus must affect the fracture. As lactose is a much softer material than calcite good grindability is expected. However, lactose is also a very elastic specimen demanding high loads until particle breakage is induced. Therefore, the comminution of lactose at comparable conditions results in relatively coarse products and large particle size distributions.

In contrast grinding of sodium ascorbate crystals which are substantially harder but also more brittle than lactose, results in finer powders with a narrow particle size distribution. This indicates that not the hardness but the elastic response of a material predominantly determines its breaking behaviour.

Sodium chloride with its very low hardness and distinct plasticity was expected to be ground to the finest milling product of all four materials: but it proved to be different. The low n -value refers to a narrow grain size distribution, whereas the high d -value indicates a large mean particle diameter.

We attribute this fracture characteristic not only to elastic–plastic properties as additional parameters like the specific density, the crystalline structure or the lattice spacing may also play a role.

The experiments affirm the hypothesis that compared with soft and inelastic materials of low density, hard and elastic materials with high specific density require enormous grinding energies.

In order to confirm the above findings and to better understand the processes in spiral jet mills, they should be described mathematically. For this purpose the milling experiments were performed according to a 3^3 factorial design. During all grinding experiments performed with different materials three operational

parameters (milling pressure, feed rate and slit width) were varied on three levels. Afterwards the results of particle size analyses (d - and n -values) taken of all milled products were evaluated statistically by means of statistical analysis system (SAS). It was shown successfully that besides the operational parameters even material properties such as hardness, young's modulus or density have significant effect on the particle size distribution of the ground product.

Moreover, it is important not to consider one singular factor solely but always to comprise the combination of material parameters. In addition other influencing variables (e.g. crystal structure) may be of importance.

The mathematical description of the grinding process is possible. By means of appropriate models the calculation of the milling conditions required to obtain a desired particle size distribution of the product is possible. Additional material properties not yet included in the calculations may have to be taken into account for further optimisation of the models. Using these improved models developed with more extensive data sets the grinding processes should be controlled more precisely.

References

- [1] M.H. Pahl, *Zerkleinerungstechnik* 2. Auflage, Fachbuchverlag, Leipzig, 1993.
- [2] H. Rumpf, *Prinzipien der Prallzerkleinerung und ihre Anwendung bei der Strahlmahlung*, Chem.-Ing.-Tech. 3 (1960) 129–135.
- [3] F. Rief, PhD thesis, University of Würzburg, 2001.
- [4] W.C. Oliver, G.M. Pharr, An improved technique for determining hardness and elastic modulus using load and displacement sensing indentation experiments, *J. Mater. Res.* 7 (1992) 1564–1583.
- [5] I.N. Sneddon, The relation between load and penetration in the axisymmetric boussinesq problem for a punch of arbitrary profile, *Int. J. Eng. Sci.* 3 (1965) 47–57.
- [6] B. Bhushan, *Handbook of Micro-nano-tribology*, second ed., CRC Press, Boca Raton, 1999.
- [7] T.Y. Tsui, G.M. Pharr, Substrate effects on nanoindentation mechanical property measurement of soft films on hard substrates, *J. Mater. Res.* 14 (1999) 292–301.
- [8] G. Simmons, H. Wang, *Single Crystals Elastic constants and Calculated Aggregate Properties: A Handbook*, second ed., The MIT Press, Cambridge MA, 1971.
- [9] K. Marquardt, PhD thesis, University of Würzburg, 2004.
- [10] M. Ramanujam, D. Venkateswarlu, *Studies in fluid energy grinding*, *Powder Technol.* 3 (1969/70) 92–101.
- [11] A. Wade, P. Weller, *Handbook of Pharmaceutical Excipients*, Washington London, second ed. 1994.
- [12] B. Bhushan, A.V. Kulkarni, W. Bonin, J.T. Wyrobek, Nanoindentation and picoindentation measurements using a capacitive transducer system in atomic force microscopy, *Phil. Mag. A* 5 (1996) 1117–1128.